Journal of Hydrology: Regional Studies 57 (2025) 102139

Contents lists available at ScienceDirect

Journal of Hydrology: Regional Studies

journal homepage: www.elsevier.com/locate/ejrh

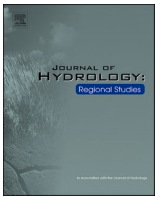

Ambient intraborehole flow in a highly productive aquifer in Ljubljana, Slovenia

Janja Svetina [a,*], Joerg Prestor [a], Simon Mozetič [a], Mihael Brenčič [b,a]

[a] Geological Survey of Slovenia, Dimičeva ulica 14, Ljubljana SI-1000, Slovenia
[b] Department of Geology, Faculty of Natural Sciences and Engineering, University of Ljubljana, Aškerčeva cesta 12, Ljubljana SI-1000, Slovenia

ARTICLE INFO

Keywords:
Borehole logging
Impeller flowmeter
Intraborehole flow
Groundwater
Ljubljansko polje

ABSTRACT

Study region: Ljubljansko polje aquifer in the central part of Slovenia.
Study focus: Impeller flowmeter was used together with the water quality probe to determine the flow characteristics of water under ambient conditions (without pumping) in 13 boreholes in a highly productive alluvial aquifer. The study focused on analysing the characteristics and variability of intraborehole flows in relation to the technical features of the boreholes, as well as the geometry and geological composition of the aquifer.
New hydrological insights for the region: The study has shown that vertical hydraulic gradients are not limited to complex multiple aquifer systems but can also occur in uniform alluvial aquifers without typical aquitard layers if hydraulic head differences exist between the upper and lower parts of the aquifer. The intraborehole flows are mainly caused by pressure-driven convection in deeper boreholes with long screens. The direction and velocity of these flows are strongly influenced by the morphology of the bedrock. Downward water flows are closely related to the local deepening of the bedrock and upward flows to the local rise of the bedrock. In some boreholes, intraborehole flow rates exceed the typical pumping rates for groundwater sampling, raising concerns about the representativeness of samples collected using conventional sampling methods. Hydrochemical logs proved to be a valuable complementary method to determine the locations of the main inflows.

1. Introduction

The installation of groundwater monitoring wells and piezometers can significantly alter natural flow dynamics and create additional pathways for potential heat and solute transport in the aquifer (Börner and Berthold, 2009). This alteration is mainly attributed to the vertical convection in the well, which can be divided into forced (pressure-forced) and free (buoyancy-driven) convection (Berthold and Börner, 2008; Eppelbaum and Kutasov, 2011).

The pressure-forced convection that occurs in groundwater monitoring wells under normal conditions, (i.e. without pumping), is usually referred to as ambient, short-circuit or cross-flow (Elçi et al., 2003; Paillet et al., 2000; Poulsen et al., 2019b). Natural factors that contribute to ambient flow in groundwater monitoring wells are vertical hydraulic gradients or hydraulic head differences, which mainly occur in groundwater recharge and discharge areas or are caused by regional drawdowns due to pumping (Börner and Berthold, 2009; Elçi et al., 2001; McMillan et al., 2014; Medici et al., 2024; Munn et al., 2020). Natural vertical hydraulic gradients are present to

* Corresponding author.
E-mail address: janja.svetina@geo-zs.si (J. Svetina).

https://doi.org/10.1016/j.ejrh.2024.102139
Received 15 October 2024; Received in revised form 4 December 2024; Accepted 13 December 2024
Available online 18 December 2024

a certain degree in almost all aquifers (Elçi et al., 2001). While these flows are generally small in undisturbed natural systems, they become non-negligible in long-screened monitoring wells, which act as a "short circuit" (Elçi et al., 2003) with a very high hydraulic conductivity (Elçi et al., 2003, 2001; Paillet et al., 1996). Ambient vertical flow in monitoring wells has been reported to occur due to head differences as small as 0.01 m between different horizons connected by the well screen (Mayo, 2010) and is likely to be greater where well screens are longer and geological layering promotes increased vertical head gradients (McMillan et al., 2014). Ambient vertical flow under static conditions depends on both the permeability of the layers and the water level difference that drives this flow (Datel et al., 2009). It acts in a gradient-dependent direction and can occur in both upward and downward direction at the same time in different sections of the water column (Börner and Berthold, 2009). The identification of ambient flow in boreholes can provide an indication of regional flow patterns (Van Meir et al., 2007).

Free convection, often referred to as natural convection, is driven by buoyancy, caused by small differences in density and hindered by viscosity as well as heat and mass diffusion (Berthold and Börner, 2008; Cermak et al., 2008; Demezhko et al., 2017). In groundwater monitoring wells, the components that influence density generally include temperature and concentration vertical gradients and their temporal variations (Berthold, 2010).

Various borehole-logging methods can be used to determine the vertical flow induced by hydraulic pressure forces, such as conventional flowmeters and high-resolution water quality probes that provide logs for one or more hydrochemical field parameters (Fricke and Schön, 1999; Kelly et al., 1993; Keys, 1997). Flowmeters can be categorised according to their basic principles into impeller, electromagnetic, heat-pulse and other tracer-release flowmeters (Keys, 1997; Molz et al., 1994). Impeller flowmeters measure the water flow rate by detecting the rotational speed of an impeller (or spinner). They are suitable for higher flow rates, where velocity is greater than 0.6 – 1.2 m/min (Kelly et al., 1993; Keys, 1997; Molz et al., 1989), as the impeller requires a certain initial velocity to start rotating. They are sensitive to mechanical disturbances caused by debris in the borehole (Newhouse et al., 2005). In contrast, electromagnetic flowmeters, which operate based on the induction, allow measurements of water flow velocities of less than 0.1 m/min (Molz and Young, 1993; Newhouse et al., 2005), heat-pulse flowmeters excel in the range of 10^{-2} m/min (Hess, 1986; Keys, 1997) and tracer-release flowmeters, which are considered the most sensitive, can detect velocities in the order of 10^{-3}-10^{-4} m/min (Hess, 1986; Keys, 1997). Flowmeter logs can be obtained in stationary or continuous mode and under ambient or pumping conditions (Paillet et al., 2000). Flowmeter data collected under pumped conditions can be used to determine the distribution of hydraulic properties in the aquifer (Molz et al., 1989; Molz and Young, 1993).

Hydrochemical logging is often performed with multiparameter water quality probes that simultaneously measure temperature, electrical conductivity, dissolved oxygen, pH and redox potential or a subset of these parameters (Schürch and Buckley, 2002). Optimal sensor resolution and a high sampling rate are important to detect small changes in the parameters, and the probe must be lowered at a slow but adequate velocity (Börner and Berthold, 2009). Temperature is the most frequently used parameter for interpreting water flow in monitoring wells. It is assumed that the monitored water temperature reflects the temperature of the surrounding rock/-sediment formation (Keys, 1997). Vertical flow disrupts the expected temperature gradient and shows little or no gradient in the affected section (Börner and Berthold, 2009). Conversely, the interpretation of electrical conductivity logs is difficult and prone to error without a thorough understanding of the flow system in the monitoring well (Keys, 1997). Although the use of additional hydrochemical parameters such as dissolved oxygen, pH and redox potential is less common in the literature, their importance in characterising aquifer properties has been demonstrated (Pauwels et al., 2015; Schürch and Buckley, 2002). The limited availability of these analyses suggests that, like electrical conductivity, they can serve as valuable complementary methods to confirm water flow conditions in monitoring wells when integrated with flowmeter and temperature logs, although their sole use to interpret intra-borehole flow is uncommon.

Understanding the characteristics of ambient vertical flow in monitoring wells is a prerequisite for assessing the representativeness of groundwater samples and in-situ measurements (Elçi et al., 2001; Poulsen et al., 2019b). Ambient vertical flows affect the water quality through heat and mass transport, which in turn affects the origin and bias of groundwater samples. Where borehole screens intersect different layers, intraborehole flows can lead to a redistribution of contaminants into uncontaminated layers. Naturally occurring intraborehole vertical flows can be an important control on the origin of samples, even in wells with screens < 10 m in length (McMillan et al., 2014). Under natural conditions, the vertical flow component has a significant influence on the geometry of the contaminant plume in groundwater and thus on the identification and localisation of contaminant sources.

The highly productive aquifer of Ljubljansko polje is the main source of drinking water for the Slovenian capital. Although the groundwater currently meets quality standards and is fed into the drinking water supply system with minimal to no treatment (Jamnik and Žitnik, 2022, 2021), the highly urbanised catchment area poses a major threat to groundwater quality (Jamnik et al., 2014; Janža, 2015). Given the previous challenges in identifying pollution sources, particularly due to spatial and temporal variations in contaminant concentrations (Svetina et al., 2024), an inconsistent sampling protocol may represent a major uncertainty leading to unrepresentative and biassed data. This concern is particularly relevant as significant vertical water flow was observed in the study area under ambient conditions.

Most previous studies conducted elsewhere have relied on a limited number of flowmeter measurements under ambient and pumping conditions to quantitatively assess the horizontal water inflows and depth-dependent hydraulic conductivity of the aquifer using different flowmeter types (Barahona-Palomo et al., 2011; Molz et al., 1989; Newhouse et al., 2005; Oberlander and Russell, 2006). In contrast, our study is one of the few that includes more than 10 measurements with a high-resolution impeller flowmeter, coupled with hydrochemical measurements, in a single highly productive alluvial aquifer with an area of about 71 km^2. The main objective of this study was to contribute to the knowledge and understanding of the characteristics and variability of intraborehole flows at the scale of a single alluvial aquifer and to provide a basis for correlating these flows with the geological composition and vertical components of groundwater flow in the aquifer. The Ljubljansko polje aquifer is of particular interest for the study of vertical

hydraulic gradients, as it is a relatively uniform, well-permeable, unconfined alluvial aquifer without typical aquitard layers. Furthermore, this study serves as the basis for a subsequent targeted sampling campaign aimed at gaining a better insight into the dynamics, transport characteristics and vertical distribution of contaminants in the boreholes and aquifer system. The specific objectives of the study were: 1. To quantify and explain the magnitude and variability of vertical intraborehole flows under ambient conditions. 2. To identify the main inflows of water along the screened sections by comparing the logs of impeller flowmeter and water quality probe. 3. To establish a methodological framework for future sampling campaigns in the study area, focussing on vertical contaminant transport in boreholes and the aquifer.

2. Study area

The study area is located in central Slovenia and comprises the alluvial aquifer of Ljubljansko polje (Fig. 1), which was formed by tectonic subsidence in the early Pleistocene (Premru and Pirc, 2005). Across the study area runs an inferred segment of a larger, active Žužemberk fault in a north-west to south-east direction (Atanackov et al., 2021) (Fig. 1), while other smaller-scale faults are also either inferred or photogeologically determined (Fig. 1) (Grad and Ferjančič, 1968; Premru, 1980).

The basin is filled with up to 100 m thick Quaternary alluvial deposits of the Sava River, consisting mainly of carbonate gravel and sand layers that are partially conglomerated and cemented with calcite cement (Janža et al., 2020; Žlebnik, 1971) (Fig. 2). Despite the presence of silt, clay and clayey gravel (Šram et al., 2012; Žlebnik, 1971), these layers occur in lens-like formations and do not represent significant aquitard layers (Fig. 2). The intergranular aquifer is therefore considered to be unconfined and relatively uniform, with the groundwater table about 20–25 m below the surface. The base of the aquifer (bedrock) consists of Carboniferous–Permian siliclastic rocks (Kolar-Jurkovšek, 2007; Premru, 1983; Žlebnik, 1971).

The average groundwater velocity is 10 m/day, although the maximum velocity can exceed 20 m/day (Janža, 2015; Janža et al., 2020). The aquifer interacts strongly with the Sava River, which recharges the aquifer in its north-western part and drains the eastern part of Ljubljansko polje (Janža, 2015; Vizintin et al., 2009) (Fig. 1, Fig. 2). Infiltration by precipitation and the Sava River contribute 2.2 m^3/s and 3.2 m^3/s of water respectively (Janža, 2015; Janža et al., 2011). Despite extensive research conducted in the past in the study area, there is currently a lack of studies evaluating the vertical hydraulic gradients under ambient conditions, particularly in relation to aquifer dynamics, transport characteristics, groundwater sampling and pollution modelling.

3. Methodology

The study was carried out between May and July 2023 under normal hydrogeological conditions. Measurements were made using a

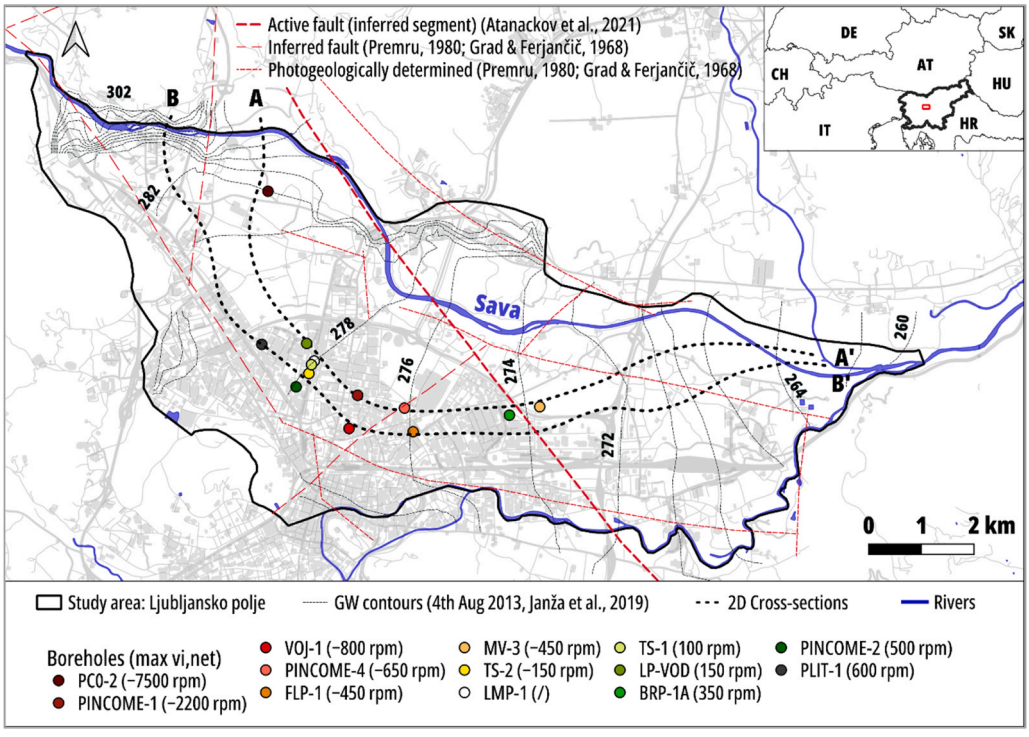

Fig. 1. Study area and the boreholes selected for the study with the absolute maximum net velocity of the impeller in revolutions per minute (rpm). This parameter is explained in detail in the following sections.

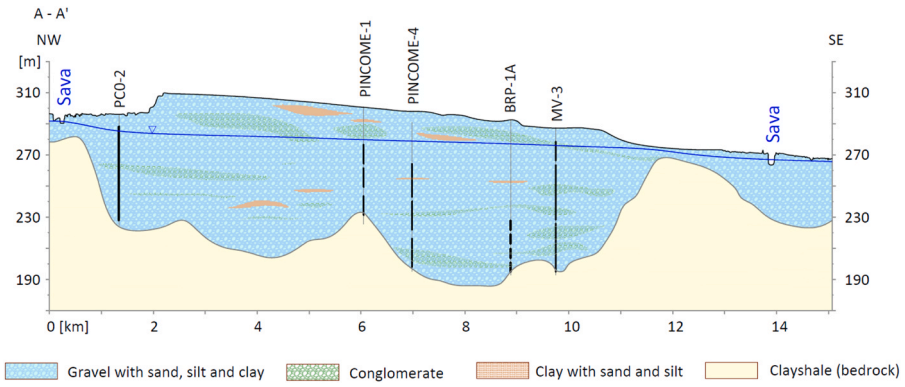

Fig. 2. Cross-section A-A′ with geological interpretation.

Water Quality probe (SWQS) for fresh water and a High Resolution Impeller Flowmeter (HRFM), both manufactured by Robertson Geologging Ltd. (Robertson Geologging Ltd.., 2024). The borehole logging was conducted in 13 piezometric boreholes (Fig. 1, Table 1). In one borehole, LMP-1, the HRFM measurement failed due to a large particle in the borehole blocking the rotation of the impeller. In addition to the measurements in 2023, two previously conducted logging experiments were included in this study (Table 1). One was conducted at the completion of the new borehole PLIT-1 in 2022, and repeated in 2023, while the second was conducted in 2018 in the borehole PC0–2. The latter was an important factor motivating our research as it revealed significant vertical water flow under ambient conditions. When selecting boreholes for this study, preference was given to deeper boreholes drilled to the base of the aquifer with accessible geological profiles, as well as boreholes located in the central part of the aquifer where better control of groundwater quality is required. All the investigated boreholes are characterised by long screen sections (Table 1), with most of them having several screen sections separated by shorter casing (non-perforated) intermediate sections. The inner diameter of most of the boreholes is 104 mm, with the exception of four boreholes. LMP-1 has a smaller inner diameter of 83 mm, while VOJ-1 and LP-VOD have larger inner diameters of 130 mm and 255 mm, respectively. Borehole MV-3 has a telescoping casing, an inner diameter of 255 mm for the first two upper screen sections and 104 mm for the third, deepest screen section.

The Water Quality probe (SWQS) contains multiple sensors that simultaneously measure the fluid properties in the aquifer (Robertson Geologging Ltd.., 2024). It provides a rapid, continuous profile of selected parameters throughout the borehole, either for direct use or as a guide for subsequent sampling. Borehole logs of temperature (°C), electrical conductivity (μS/cm) and dissolved oxygen (ppm and %) were recorded. The fluid properties were always recorded prior to logging with the flowmeter, and always in the downhole direction to minimise disturbance to the fluid properties. The logging speed was between 1.5 and 2 m/min and did not exceed the recommended maximum speed of 3 m/min (Robertson Geologging Ltd.., 2024) as the sensors are moderately slow to respond to changes in the borehole fluid.

The High Resolution Impeller Flowmeter (HRFM) has a lightweight, helical impeller mounted on double sapphire bearings (Robertson Geologging Ltd.., 2024). As the fluid moves through and rotates the blades of the impeller, the number of impeller revolutions per minute (rpm) is automatically recorded. The flowmeter head is a precision mechanism with very low friction that can

Table 1
The boreholes selected for the study, their depth, the length of the screen sections, the date of borehole logging and the methods used.

No	Borehole	Year of construction	Bor. depth (Aq. base)	Length of screen sections	Date	Methods used
1	PINCOME−4	2011	96 (94)	21 + 18 + 18	05/04/23	HRFM, SWQS
2	VOJ−1	2014	114.6 (111)	14 + 38	07/04/23	HRFM, SWQS
3	FLP−1	2004	106 (104.2)	21 + 18 + 18	12/04/23	HRFM, SWQS
4	PINCOME−1	2010	75.2 (68)	*3* × 12	17/04/23	HRFM, SWQS
5	MV−3	1997	94.5 (91.6)	12 + 35 + 31	24/04/23	HRFM, SWQS
6	LMP−1	2006	93 (90)	16 + 24	05/05/23	SWQS
7	BRP−1A	2004	99 (97)	*4* × 6	09/05/23	HRFM, SWQS
8	PINCOME−2	2011	68 (66)	18 + 18	22/05/23	HRFM, SWQS
9	TŠ−1	2011	40 (/)	16	30/05/23	HRFM, SWQS
10	TŠ−2	2011	40 (/)	16	30/05/23	HRFM, SWQS
11	PLIT−1	2022	92 (/)	*11* × 5	04/07/23	HRFM, SWQS
12	LP-VOD	1977	54.8 (/)	11.5 + 10	14/07/23	HRFM, SWQS
13	PLIT−1	2022	92 (/)	*11* × 5	23/05/22	HRFM, SWQS
14	PC0–2	2018	74 (71.5)	60	09/11/18	HRFM, SWQS, DTR 65 HRCF-MPX

Notes: HRFM: High-resolution impeller flowmeter; SWQS: Water Quality probe for fresh water; DTR 65 HRCF-MPX: borehole TV camera inspection system; Bor. Depth: Borehole depth; Aq. Base: Aquifer base; (/): Data unknown.

reliably rotate at a speed as low as 1 m/min (Robertson Geologging Ltd.., 2024). The head carries a toroidal magnet with four poles around its circumference. A pair of Hall-effect sensors are used to determine both the speed and direction of rotation. Four pulses are counted for each revolution. Impeller performance at low flow rates is limited by the force required to rotate the impeller and at high flow rates turbulence causes the rotation speed to deviate from ideal values (Robertson Geologging Ltd.., 2024).

For the impeller flowmeter (HRFM) tests, a standard continuous logging procedure (Keys, 1990) was used where a device was run down and up in a static fluid (without pumping) at different line cable trolling velocities (v_c) to measure the ambient flow in the borehole. The runs were carried out at line cable velocities of 4, 5, 7 and 9 m/min respectively. Exceptions are the measurements previously carried out in PLIT-1 in 2022 and PC0–2 in 2018 at line cable velocities of 3, 5, 7 and 9 m/min for PLIT-1 and 3, 5, 7 and 10 m/min for PC0–2. The flowmeter was always used together with a “bow spring” centraliser that aligns and protects the impeller.

The impeller flowmeter measures the rotational velocity of the impeller $v_{i(c)}$ (rpm), which is influenced by two main factors: the velocity of line cable trolling v_c (m/min) and the velocity of intraborehole water flow v_w (m/min) (Sellwood et al., 2015). Both the velocity of the impeller $v_{i(c)}$ and the velocity of line cable trolling v_c are bidirectional (Hearst et al., 2000), while the intraborehole water flow v_w can also be deflected in directions other than vertical due to inflows in screened sections. However, in the context of our study, the focus is mainly on the vertical direction, where the term "vertical" refers to both directions – up and down. If we want to specify only one direction of a parameter, we name it accordingly, e.g. up or down, or use the corresponding sign. A negative sign was assigned for the downward direction and a positive sign for the upward direction. As the manufacturer uses the convention where v_c is negative when moving uphole (Robertson Geologging Ltd.., 2024), all raw measurements of $\vec{v}_{i(c)}$ were multiplied by −1 to ensure consistency of processing.

3.1. Impeller flowmeter calibration

The vertical velocity of intraborehole water flow (v_w) can be determined by calibration, i.e. by plotting the measured impeller velocities $v_{i(c)}$ (rpm) against the line cable velocities v_c (m/min) (Keys, 1990). However, such a calibration is only valid for the cased (non-perforated) sections of the borehole (Berthold and Börner, 2008; Hearst et al., 2000; Keys, 1990; Oberlander and Russell, 2006; Robertson Geologging Ltd.., 2024). The calibration of the probe should be carried out at different line cable velocities, separately for downward and upward runs, and the resulting correlation should be linear (Robertson Geologging Ltd.., 2024) in the following form:

$$v_{i(c)(rpm)} = a_x * v_{c(m/\min)} + b_x \tag{1}$$

The coefficients a_x and b_x were determined in our study based on a linear regression, where a_x is the slope of the regression line and b_x is the y-intercept of the regression line. The subscript x indicates the direction of v_c in which the calibration was performed and is shown in the results as subscript d for the downward direction and as subscript u for the upward direction. Fig. 3 shows two examples of calibration - in a static fluid (a) and in a section with downward ambient water flow (b). The dashed linear line represents an ideal response for a frictionless impeller, where any fluid velocity would cause rotation. The solid lines, on the other hand, show that the fluid must pass through the impeller at significant velocities before it begins to rotate (Keys, 1990; Robertson Geologging Ltd.., 2024). Therefore, the actual HRFM measurements require separate calibration for the downward and upward runs.

The points of intersection with the *x-axis*, labelled v_d and v_u, are the threshold velocities or the lowest flow velocities required to set the impeller in motion in the downward and upward directions of borehole logging respectively (Keys, 1990; Robertson Geologging Ltd.., 2024). The threshold velocity of the HRFM used is 1 m/min, as specified by the manufacturer (Robertson Geologging Ltd.., 2024). However, the threshold velocities are not necessarily identical (Keys, 1990). According to (Robertson Geologging Ltd.., 2024), the upward slope may be shallower than the downward response slope because the tool body shields the impeller to a certain degree

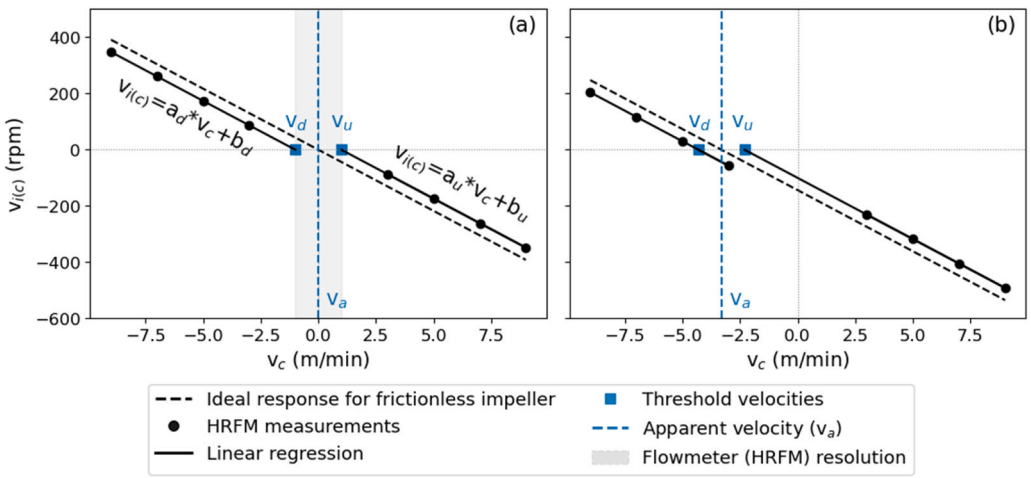

Fig. 3. An example of impeller calibration in a static fluid (a); An example of impeller calibration in the section with the downward water flow (b).

during upward runs. The midpoint between v_d and v_u gives the apparent vertical water velocity v_a in this section of the borehole (Robertson Geologging Ltd.., 2024).

Calibration was performed for the boreholes listed in Table 1, where either negligible or significant vertical flow was detected in the non-perforated casing section. No inflows are expected here unless the casing is damaged (e.g. cracked plastic or corroded iron), the casing joints are leaking or the non-perforated sections are exceptionally short.

3.1.1. Quantifying vertical component of groundwater flow within borehole

As the flow rate is highest in the centre of the borehole and decreases towards the edges, a correction factor must be used. Depending on the size of the impeller compared to the pipe diameter, this factor can be between 0.75 and 0.9 (Sondex, 2007). The correction factor of 0.83 was used in accordance with the value accepted in the industry (Sondex, 2007). To calculate the production rate, the radius of the borehole should be taken into account by using Eqs. (2) and (3):

$$v_w = 0.83 * v_a \tag{2}$$

$$Q = \pi r^2 * v_w \tag{3}$$

Where v_a is the apparent vertical water velocity (m/min), v_w is the vertical water velocity (m/min), Q is the vertical water flux (m^3/min) and r(m) is the borehole radius.

3.2. Interpretation of borehole logs

The logs of impeller velocities $v_{i(c)}$ (rpm) from the downward and upward logging of the same speed (e.g. $v_{i(c)}$ (rpm) recorded with both upward and downward logging at 5 m/min) were summed according to Eq. (4). In this way, the contribution of the cable trolling velocity v_c is removed and the distribution of the net impeller velocity $v_{i(c),net}$ (rpm) over depth is obtained, which is proportional to the vertical intraborehole flow. The negative values of $v_{i(c),net}$ indicate a downward water flow, while positive values of $v_{i(c),net}$ indicate an upward water flow. If $v_{i(c),net}$ is equal to 0 or fluctuates very close to 0, it is assumed that the water in the borehole is at a standstill or that the vertical water flow is negligible.

$$v_{i(c),net} = v_{i(c),down} + v_{i(c),up} \tag{4}$$

The (net) velocities of the impeller are stated exclusively in revolutions per minute (rpm) in this paper, as this is the only unit that reliably represents measurements over the entire borehole depth. The conversion to vertical velocity of intraborehole flow v_w (m/min), the main parameter of interest, is only reliable in short calibration sections where the borehole casing is not perforated.

Abrupt changes in $v_{i(c),net}$ at very short intervals may indicate localised stronger inflows, changes in the alignment of the flowmeter within the borehole casing or occasional debris impacts. A strong indication of inflow is assumed if the abrupt shifts in $v_{i(c),net}$ are accompanied by significant changes in one or more hydrochemical parameters such as temperature, electrical conductivity or dissolved oxygen. Therefore, the water quality probe logs were plotted against depth together with $v_{i(c),net}$ values to identify such locations.

In general, the interpretation of flowmeter measurements is further complicated by factors such as friction in the impeller bearings, the viscosity of the fluid, turbulence caused by the movement of the probe, inadequate centralisation, the inclination of the borehole and the actual flow velocity profile in the boreholes (Robertson Geologging Ltd.., 2024). If both - the direction and the velocity - of the intraborehole flow (v_w) and the line cable trolling (v_c) are the same, the flow past the impeller is not sufficient to cause rotation, so the impeller stalls (Oberlander and Russell, 2006). This is also the case when the directions of water and line cable trolling are the same and the absolute velocity difference between v_w and v_c is less than the resolution of the impeller flowmeter. When interpreting the measurements in such a case, attention must be paid to whether the velocity and direction of the impeller logging and the water flow really match or whether the impeller could be blocked for another reason, for example by suspended particles in the borehole.

3.3. Hydrogeological interpretation

3.3.1. Borehole characteristics

For all boreholes included in the analysis, the geological profiles were gathered, which contain a more or less detailed geological inventory of the ground. As the profiles were prepared by different contractors at different times, the geological inventories are inconsistent and differ both in their accuracy and in the way the sediments are described or classified. As part of the study, we reviewed all available data and reclassified the sediments according to the ISO standard (SIST EN ISO 14688–2:2004, 2004) based on the content of gravel (Gr), sand (Sa), silt (Si) and clay (Cl). The texture classes were further interpreted and grouped with respect to the expected relative range of permeability of the sediments (Domenico and Schwartz, 1998). In addition, the technical information on the borehole casing, including data on the diameter, length and depth of the screen sections, was compiled. This was crucial for the correct interpretation of the borehole logging data.

3.3.2. Vertical gradient of groundwater flow within aquifer

One of the piezometric boreholes, BRP-1A, is part of a monitoring well cluster consisting of three adjacent monitoring wells (BRP-1A, BRP-1B and BRP-1C), each equipped with screen sections at different depths in the subsurface. Although the borehole logging was

only conducted in the deepest borehole, BRP-1A, the hydraulic head was measured several times simultaneously in all three boreholes to capture potential differences in hydraulic head.

3.3.3. Geometry of the aquifer

Using QGIS, two 2D cross-sections A-A' and B-B' (Fig. 1) were created along the projected groundwater streamlines obtained from an existing hydrogeological numerical model (Janža et al., 2020, 2011) to improve our understanding of the aquifer heterogeneity and its connection with the borehole logging results. The surface topography was determined from publicly available LiDAR imagery (ARSO, 2024) and the base of the aquifer was extracted from an interpolated raster layer (Janža et al., 2017).

3.3.4. Groundwater characteristics

It is generally assumed that the temperature measured in a monitoring well represents the temperature of the surrounding geological formation (Börner and Berthold, 2009). In general, the temperature gradients in the shallow zone are influenced by seasonal fluctuations, while in the deeper zones they are governed by the geothermal gradient. Hydrochemical parameters such as electrical conductivity, dissolved oxygen, pH and Eh serve primarily as supplementary indicators of both prominent horizontal inflows and notable vertical flows. Horizontal inflows manifest as abrupt shifts in one or more parameters, while parameters that remain constant over longer depth sections strongly indicate the presence of significant vertical flows and provide valuable insights into the dynamics of the flow in the monitoring wells.

4. Results

4.1. Impeller flowmeter logs

Borehole logging with the impeller flowmeter was successfully carried out in 12 different boreholes, 13 times in total, whereby the measurements in PLIT-1 were repeated twice, one year apart. Fig. 4a shows an example of an impeller flowmeter log from borehole VOJ-1 with 8 curves representing the impeller response $v_{i(c)}$ measured at different line cable trolling velocities (v_c) of 4, 5, 7 and 9 m/min in the downward and upward directions respectively. The fluctuations of flowmeter logs can be observed at different scales (Fig. 4a). The first scale (1.) is the measurement noise, which reflects small fluctuations due to minor changes in line cable trolling velocity and short recording intervals. Other influences such as localised stronger horizontal inflows that can cause flow turbulence, changes in the alignment of the flowmeter within the borehole casing and occasional debris impacts can cause fluctuations on a small to medium scale (2.). Indications of vertical water direction are only observed at a larger scale of a few metres to a few tens of metres where consistent deviations of the curve occur (3.). The intervals where the impeller response curves appear as straight lines indicate the stall of the impeller (e.g. $v_{i(5),down}$ between 75 and 110 m depth). In these intervals, it is assumed that the direction and velocity of v_c is approximately the same as the direction and velocity of v_w or that the absolute difference between v_c and v_w is less than the resolution of the impeller flowmeter, unless the impeller is blocked for other reasons (e.g. by larger suspended matter).

Fig. 4b shows the net impeller velocities $v_{i(c),net}$ (rpm) calculated according to Eq. (4). The net impeller velocity curves are generally

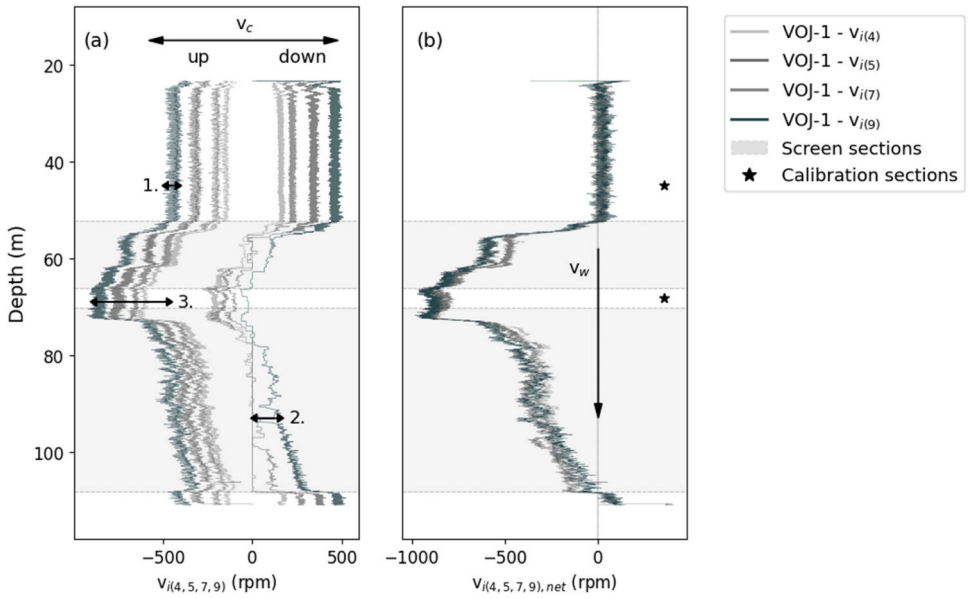

Fig. 4. Example of an impeller flowmeter log from borehole VOJ-1 with characteristic scales of fluctuation (a); interpretation of the downward intraborehole flow in borehole VOJ-1 (b).

well aligned, except between 55 and 62 m depth, where the deviations of the individual curves reflect the stalls of the impeller. In the upper casing section between 20 and 50 m depth, the intraborehole flow is negligible (≈ 0 rpm), while in the screen sections we can observe the general deviation of $v_{i(c),net}$ towards the negative rpm values, indicating a downward intraborehole flow. The downward velocity of the water appears to be strongest between 68 and 70 m.

Considerable variability in the direction of water flow was observed between the different boreholes (Fig. 5). Six boreholes exhibited pronounced downward flow in certain depth segments, with the most notable maximum of $v_{i,net}$ observed at PC0–2 (-8000 rpm) and PINCOME-1 (-2200 rpm). Boreholes VOJ-1, PINCOME-4, FLP-1 and MV-3 exhibited $v_{i,net}$ between −800 and −450 rpm. In contrast, only three boreholes showed a characteristic upward flow of water at certain depths: PLIT-1, PINCOME-2 and BRP-1A, with $v_{i,net}$ values between 350 and 600 rpm. Smaller, insignificant vertical flows were observed at TŠ-1, TŠ-2 and LP-VOD (+/- 150 rpm). In 7 boreholes, namely PLIT-1, PINCOME-2, PINCOME-1, VOJ-1, PINCOME-4, FLP-1 and MV-3, significant stalling of the impeller occurred at certain velocities and logging directions.

4.1.1. *Impeller flowmeter calibration*

An example of the calibration of impeller flowmeter is shown in Fig. 6. The absolute threshold velocities v_d and v_u in the VOJ-1 borehole section between 40 and 50 m depth are about 1.5 m/min (Fig. 6a), which agrees relatively well with the threshold velocity of 1 m/min specified by the manufacturer of the HRFM (Robertson Geologging Ltd.., 2024). The apparent vertical velocity of the water was estimated to be 0.08 m/min in this depth interval, which is considered negligible. In contrast, a significant downward vertical flow of −8.65 m/min was observed in the non-perforated cased section of borehole VOJ-1 at 68–70 m depth (Fig. 6b).

All borehole depth segments considered for the calibration and the corresponding estimated parameters are listed in Table 2. The calibration was not performed for boreholes PC0–2, TŠ-1 and TŠ-2, which are only equipped with a screen section over the entire borehole depth and are therefore not suitable for calibration. The negligible vertical water flow was observed at certain depths of VOJ-1, BRP-1A, PLIT-1, PINCOME-2, PINCOME-4 and FLP-1 (Table 2), where the mean $v_{i,net}$ was close to 0 rpm (+/- 30 rpm). At these sections, the linear regression coefficients are relatively consistent, with small deviations (Fig. 6c, Table 2). The mean slope for downward runs (a_d) is −56.2 with a standard deviation of 4.1, while the mean slope for upward runs (a_u) is −56.9 with a standard deviation of 3.6. The overall median value of slope is −59.2 for downward runs and −57.6 for upward runs.

Larger deviations in the linear regression coefficients occur when calibrating measurements where a characteristic vertical flow occurs, i.e. a significant deviation to more positive or more negative $v_{i,net}$ values (Fig. 6c, Table 2). This is particularly true for the coefficient *b* or the intercept with the *y-axis*, which reflects the apparent vertical velocity v_a (Table 2, Fig. 6c). On the other hand, larger deviations in the linear regression slope may indicate changes in the alignment of the impeller flowmeter during the measurements or the possible presence of a horizontal water component or the turbulence. Therefore, the correlation between the mean net impeller velocity $v_{i,net}$ (rpm) and the vertical water flow v_w (m/min), calculated according to Eq. (2), was verified. A significant positive correlation was found with an r-value of 0.987 and a p-value of 1.84×10^{-16} (Fig. 7a).

The simultaneous measurements of hydraulic head in the monitoring well cluster (BRP-1A, BRP-1B and BRP-1C) showed that the borehole with the deepest screens, BRP-1A, has a higher hydraulic head than the shallower BRP-1B and BRP-1C (Fig. 7b). Based on five measurements between June 2023 and March 2024, the hydraulic head in BRP-1A is on average 4.5 cm higher than in BRP-1B and 4.6 cm higher than in BRP-1C, which has the shallowest screens. The difference between BRP-1B and BRP-1C is therefore only 0.1 cm and is relatively stable, as the same result was measured for all five measurements. On the other hand, the difference between BRP-1A and BRP-1B varies between 2.6 and 5.6 cm. These differences could to some extent be a result of measurement errors, but they can also

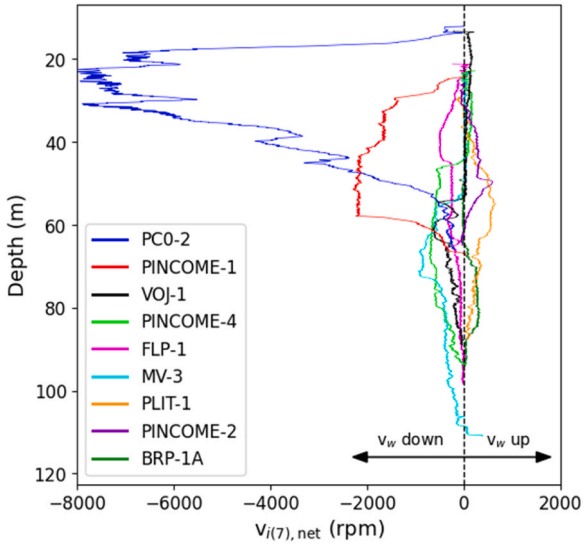

Fig. 5. Comparison of 9 boreholes with clearly identified intraborehole flow.

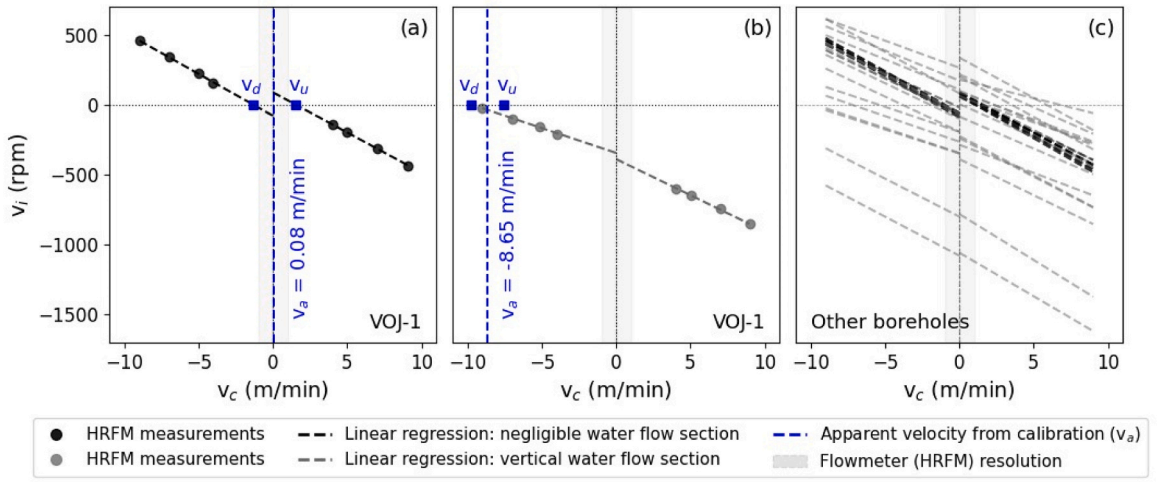

Fig. 6. Example of the calibration of impeller flowmeter at VOJ-1: cased section with negligible flow at 40–50 m depth (a) and cased section with significant vertical flow at 68–70 m depth (b); comparison of the linear regression lines from the calibration of impeller flowmeter in different boreholes (c).

Table 2
Impeller flowmeter calibration.

Borehole	Depth *m*	Mean $v_{i,net}$ *rpm*	a_d	a_u	b_d	b_u	v_d *m/min*	v_u *m/min*	v_a *m/min*	Q_w *l/s*
VOJ−1	40–50	20	−59.8	−57.4	−80.6	86.9	−1.35	1.51	0.08	0.015
BRP−1A	55–60	−7	−59.2	−60.7	−59.2	63.1	−1.00	1.04	0.02	0.002
PLIT−1/22	31–32	−21	−59.3	−60.7	−92.8	78.6	−1.57	1.30	−0.14	−0.02
PLIT−1/23	31–32	−11	−49.8	−57.6	−21.0	60.5	−0.42	1.05	0.31	0.04
PINCOME−2	26–27	30	−50.5	−49.9	−66.0	53.5	−1.31	1.07	−0.12	−0.01
PINCOME−4	25–27	26	−59.7	−58.3	−65.5	82.3	−1.10	1.41	0.16	0.02
FLP−1	21–24	21	−54.9	−53.9	−65.7	87.1	−1.20	1.62	0.21	0.03
VOJ−1	68–70	−836	−35.5	−51.6	−346.2	−390.1	−9.74	−7.57	−8.65	−1.59
BRP−1A	80–82	288	−59.0	−58.1	79.6	201.9	1.35	3.48	2.41	0.29
PLIT−1/22	61–62	386	−43.2	−45.8	170.3	237.5	3.95	5.82	4.88	0.57
PLIT−1/23	61–62	514	−38.8	−26.7	262.3	178.9	6.76	6.69	6.73	0.79
PINCOME−2	45–48	298	−42.2	−45.3	113.8	202.2	2.48	4.57	3.52	0.41
PINCOME−4	70–75	−591	−24.4	−40.2	−205.5	−287.3	−7.27	−7.14	−7.21	−0.85
FLP−1	50–55	−260	−53.3	−45.7	−221.6	−86.6	−3.87	−1.90	−2.89	−0.34
FLP−1	80–85	−76	−50.9	−47.4	−102.3	3.8	−2.01	0.08	−0.96	−0.11
PINCOME−1	37–40	−1654	−54.3	−65.6	−801.2	−782.6	−14.75	−11.93	−13.34	−1.57
PINCOME−1	52–58	−2179	−55.8	−62.2	−1080.4	−1058.7	−19.35	−17.02	−18.19	−2.14
LP-VOD	28–30	84	−53.9	−37.2	−79.2	57.9	−1.47	1.56	0.05	0.03
LP-VOD	42–45	127	−56.1	−39.3	−67.4	89.4	−1.20	2.27	0.54	0.38
MV−3	21–24	115	−55.2	−43.4	−57.8	98.8	−1.05	2.28	0.62	0.43
MV−3	59–61	−547	−35.6	−56.4	−194.7	−224.7	−5.47	−3.98	−4.73	−0.17

Notes: a_d, b_d: Calibration coefficients for the downhole borehole logging, determined using Eq. (1), where a_d is the slope of the linear regression line and b_d is the intercept with the y-axis; a_u, b_u: Calibration coefficients for the uphole borehole logging, determined using Eq. (1), where a_u is the slope of the linear regression line and b_u is the intercept with the y-axis.

be attributed to different hydrogeological conditions. In general, the results agree well with the interpretation of the vertical upward water flow in the deepest borehole, BRP-1A. The upward ambient flow in the borehole is a consequence of hydraulic pressure, which is higher in the lower part of the aquifer.

4.1.2. Comparison of borehole logs in PLIT-1 in 2022 and 2023

A comparative analysis of the flowmeter logs from 2022 and 2023 shows a consistent upward direction of water flow in both years, particularly within the 49–62 m depth segment. The vertical flow is evidenced both by the flowmeter logs, which can be seen as a shift towards the positive $v_{i.net}$ rpm values (Fig. 8b), and by the temperature (Fig. 8c) and electrical conductivity (Fig. 8d) logs, where an almost straight line with negligible changes in parameter values can be seen in the segment between

43–62 m depth. In addition, a significant phenomenon of stalling of the impeller is observed during the response of the impeller in

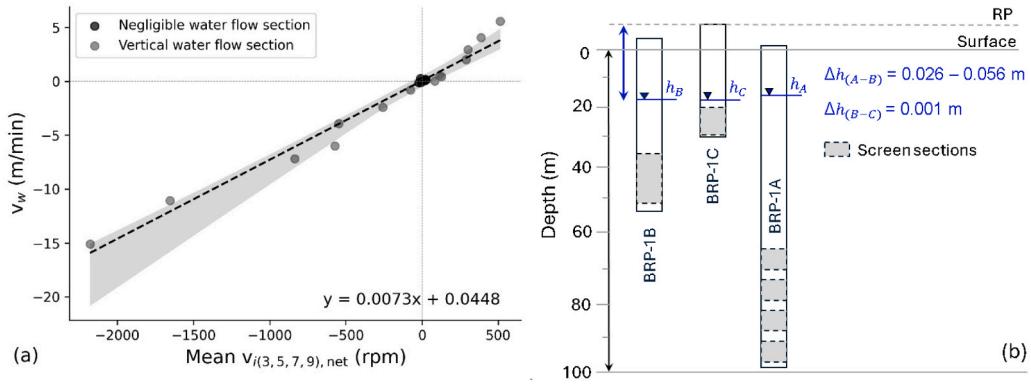

Fig. 7. Correlation of the mean $v_{i,net}$ (rpm) with the calculated v_w (m/min) with 95 % confidence interval for the segments from Table 2 (a); graphical representation of the hydraulic head in the monitoring well cluster – BRP-1A, BRP-1B and BRP-1C (b).

2023 to an upward logging velocity v_c of 7 m/min (Fig. 8a), which can be interpreted as additional confirmation of the upward direction of water flow in the borehole.

Fig. 8a shows that the impeller response v_i, recorded at a v_c of −7 m/min and 7 m/min, agrees well between the two years in the upper (30–40 m) and lower sections (75–90 m) of the borehole. However, there are differences in the middle section, where the vertical water flow is most pronounced. This is particularly evident in the $v_{i,net}$ response (Fig. 8b), which indicates that the vertical water velocity is higher in 2023 than in 2022. A comparison of $v_{i(7),net}$ and $v_{i(9),net}$ response curves (Fig. 8b) shows that this observation is not distorted by the stall of the impeller between 51 and 61 m in 2023 while logging up with v_c of 7 m/min (Fig. 8a). In fact, the two curves of $v_{i(7),net}$ and $v_{i(9),net}$ overlap very well in this middle section (Fig. 8b) and no bias is expected as no stall of the impeller was observed while logging up with v_c of 9 m/min. Similarly, the calibration of the impeller flowmeter in sections 61–62 (Table 2) showed that the apparent velocity v_a of the vertical water flow in 2022 was about 1.8 m/min lower than in 2023.

The PLIT-1 borehole is cased with 11 screen sections, each 5 m long, with 1 m long non-perforated sections in between (Fig. 8b). It can therefore be assumed that horizontal water inflows occur along the entire borehole where screens are present. However, some potentially stronger horizontal inflows have been interpreted, where abrupt changes in $v_{i(c),net}$ are accompanied by significant changes

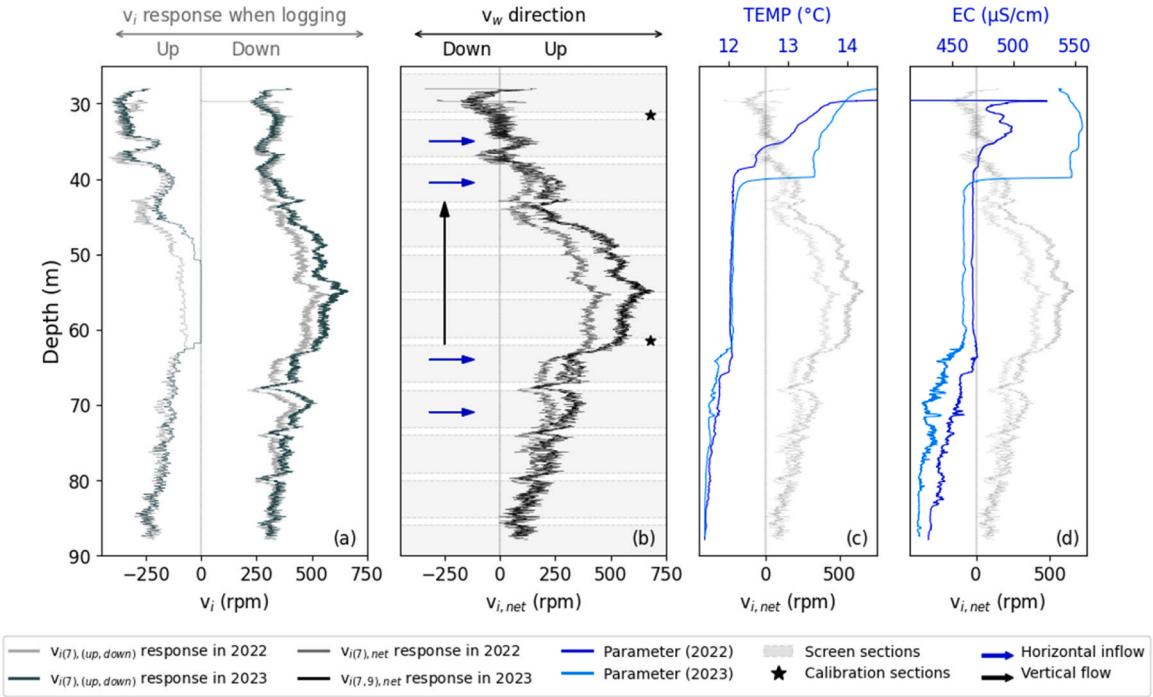

Fig. 8. Comparison of the impeller flowmeter logging in PLIT-1 in 2022 and 2023. The response of the impeller flowmeter in the downward and upward direction of logging at the velocity of 7 m/min in 2022 and 2023 (a); the net velocity of impeller flowmeter in 2022 and 2023 (b); the temperature (TEMP) and electroconductivity (EC) in 2022 and 2023 (c,d).

in temperature and/or electrical conductivity. This is mainly observed at 40 and 64 m depth, but also at 35 and 71 m depth (Fig. 8b, Fig. 8c, Fig. 8d).

4.2. Water quality probe logs

The groundwater temperature in boreholes ranged from 11.3 to 16.2 °C with an average value of 12.7 °C (Table 3). The results of the quality probe logs show that temperature generally decreases with depth, especially where significant horizontal water inflows were observed (Fig. 8c). The highest standard deviation was observed in LMP-1, PINCOME-2, PLIT-1, TŠ-1 and LP-VOD (Table 3). The anomalies of higher temperature occur here mainly in the upper 3–15 m of the groundwater column. In LMP-1 and LP-VOD, the anomaly is located in the cased, non-perforated section of the borehole with more or less stagnant water, and the water temperature typically changes at the transition to the screen section due to the inflow of fresh groundwater. In contrast, for PINCOME-2, PLIT-1 and LP-VOD, the higher water temperature anomaly is also characteristic of the upper part of the screen section, where fresh groundwater is already flowing in, which could indicate anthropogenic heat sources in the urban area.

The electrical conductivity ranged from 283 to 678 μS/cm with an average value of 432 μS/cm (Table 3). Borehole PC0–2 is characterised by significantly low electrical conductivity values below 300 μS/cm. However, significantly high values only occur locally, as observed in PINCOME-2 within the upper 5 m of the groundwater column, where the electrical conductivity is more than 300 μS/cm above the average value in the borehole. In general, electrical conductivity shows very similar patterns to temperature, particularly in relation to the locations of anomalies and the sections with consistent values.

Several boreholes are characterised by more or less long sections along the depth where the changes in hydrochemical parameters along the depth are negligible. Two examples are shown in Fig. 8 and Fig. 9. While an upward vertical flow was observed in PLIT-1 (Fig. 8b), downward vertical flow is significant in PINCOME-1 (Fig. 9b). The PINCOME-1 borehole is cased with 3 screen sections, each 12 m long. In between are 2 shorter, non-perforated sections of 3 and 6 m in length (Fig. 9). Based on the flowmeter log, a significant downward water flow occurs almost imidiately at the transition into the first screen section and becomes the most pronounced in the second screen section around 44 m depth. This pattern continues through the second non-perforated section between 51 and 57 m and changes significanly at the transition in the third screen section at 57 m depth. The downward vertical flow is still present here, but continuously decreases towards the bottom of the borehole. The siginificant vertical flow is also seen from the hydrochemical logs, by negligible changes in temperature, electrical conductivity and dissolved oxygen in the same interval (Fig. 9).

However, where abrupt changes in $v_{i(c),net}$ are accompanied by significant changes in temperature and/or electrical conductivity, potentially stronger horizontal inflows were interpreted. This is particularly evident at around 28 m depth, where we observe anomalies in temperature, electrical conductivity and dissolved oxygen. However, in the third screen section, where the flowmeter indicates the discharge of water flowing from the upper parts of the borehole, the temperature and electrical conductivity do not change, but dissolved oxygen shows some minor anomalies, particularly at about 61 m depth.

4.3. Hydrogeological interpretation

Determining the phenomena of the main inflows into the boreholes and the characteristics of intraborehole flows from a geological perspective is generally challenging for two main reasons. Firstly, the geological data comes from different sources with various classification systems and different degrees of accuracy, which can be misleading. The resolutions range from precise measurements with an accuracy of 10 cm in some places to rather coarse inventories covering sections of several tens of metres in other places. Secondly, the representation of the different geological formations is unevenly distributed. Fig. 10 shows that vertical flows occur both

Table 3
Minimum, maximum, mean and standard deviation of temperature (°C) and electrical conductivity (μS/cm) in the boreholes.

	Temperature (°C)				Electrical conductivity (μS/cm)			
Borehole	Tmin	Tmax	Tmean	Tstd	ECmin	ECmax	ECmean	ECstd
BRP−1A	11.9	12.7	12.1	0.2	386.7	402.9	395.9	4.4
FLP−1	12.8	13.3	13.1	0.1	436	457.1	449.8	6.6
LP-VOD	11.5	13.5	11.7	0.5	389.9	420	394.2	6.6
MV−3	12.6	13.3	13	0.1	440.1	481.7	463	12.0
PINCOME−1	12.6	12.8	12.7	0.0	471.9	479.5	473.5	1.5
PINCOME−2	11.6	16.2	12	1.0	309.3	677.1	367.9	110.9
PINCOME−4	12.1	12.8	12.8	0.1	475.7	493.5	486.9	2.0
PLIT−1	11.6	14.6	12.2	0.8	421.2	556.5	465.7	44.5
PLIT−1/22	11.6	14.3	12.1	0.5	430.3	527.5	460.9	18.3
VOJ−1	12.7	13.9	13.5	0.3	461.4	503.3	478.6	13.7
PC0–2	12.6	12.8	12.7	0.1	282.9	291.1	283.9	45.9
TŠ−1	13.4	15.5	14.6	0.6	333.7	498.1	410.8	51.3
TŠ−2	13.4	14	13.5	0.1	486.4	535.1	522.4	8.9
LMP−1	11.3	15.4	11.8	1.2	295.6	411.5	389.1	26.5
Min	11.3	12.7	11.7		282.9	291.1	283.9	
Max	13.4	16.2	14.6		486.4	677.1	522.4	
Mean	12.3	14.0	12.7		401.5	481.1	431.6	

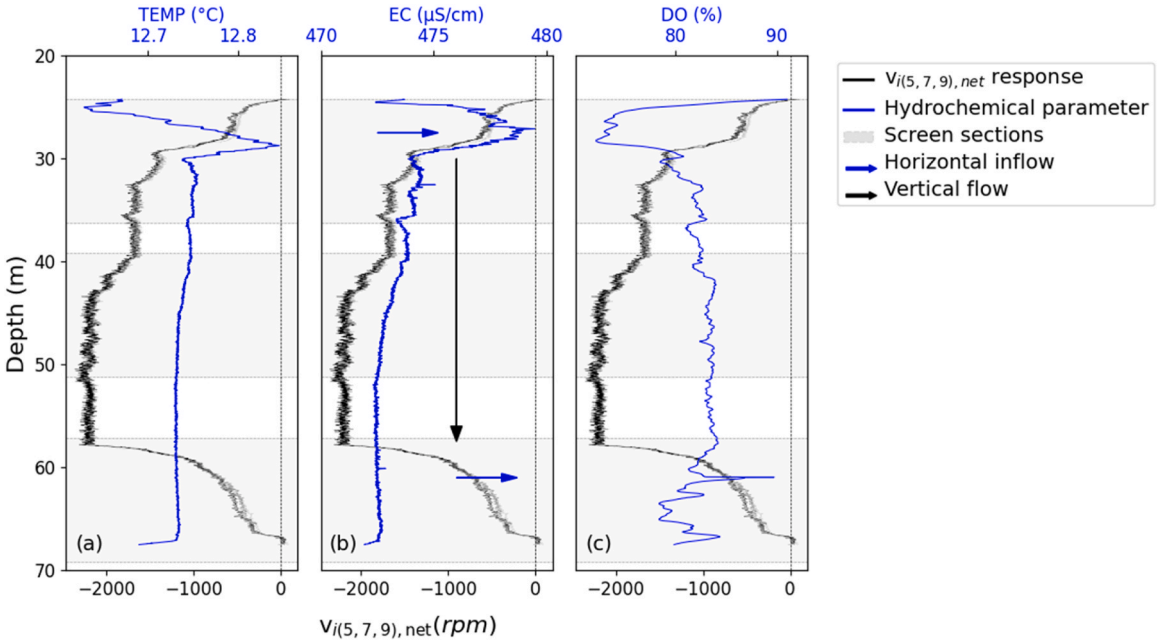

Fig. 9. Combined analysis of flowmeter and hydrochemical logs in PINCOME-1.

in boreholes with significant differences in alluvial sediment composition (e.g. PLIT-1 and VOJ-1), as well as in those with very uniform alluvial sediment composition, where only minimal differences in soil permeability are expected (e.g. PINCOME-1 and FLP-1). The analysis also does not indicate that the direction of vertical water flow in the boreholes is related to any specific sequence of sediment layers.

However, based on the two cross sections through the aquifer along the main groundwater flowlines, it was determined that the

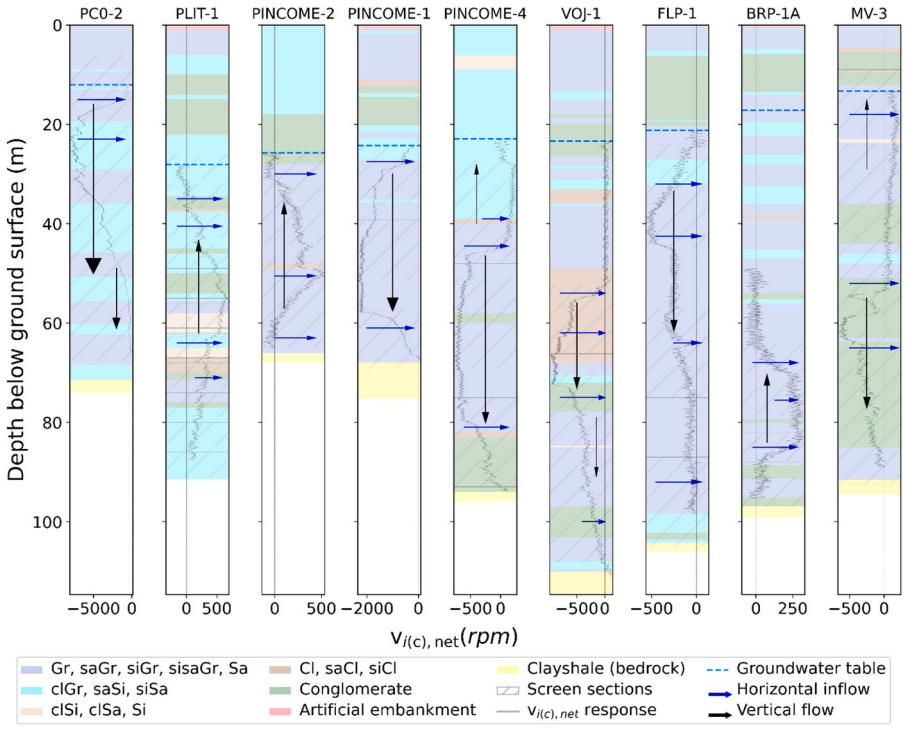

Fig. 10. Hydrogeological interpretation of the borehole geological inventory of the ground with directions of vertical intraborehole flow and locations of potentially stronger inflows.

intraborehole vertical flows are primarily related to the shape of the bedrock (i.e. the base of the aquifer with low permeability) (Fig. 11). The absolute maximum values of the net impeller velocities were below 800 rpm in most of the boreholes, in contrast to PINCOME-1 and PC0–2, which stand out with absolute values of 2200 and 7500 rpm respectively (Fig. 5). When analysing the two cross-sections through the aquifer (Fig. 11), a common feature of PC0–2 and PINCOME-1 becomes clear: both are located before the deepening of the bedrock. While PC0–2 is located in the intensive recharge zone from the Sava River, adjacent to the primary initial deepening of the bedrock, PINCOME-1 is located in the central part of the aquifer. The discernible downward vertical water flow, albeit only a third of that observed at PC0–2, is likely a consequence of its location near the local maximum of the bedrock, followed by subsequent re-deepening of the bedrock in a downgradient direction. Similarly, the minor downward water flow observed in boreholes PINCOME-4, MV-3 and VOJ-1 is associated with the local deepening of the bedrock, while the minor upward flow observed in BRP-1A, PLIT-1 and PINCOME-2 is associated with the local rising of the bedrock (Fig. 11).

There are certainly some deviations that require explanation. Although PINCOME-2 reaches the bottom of the aquifer, its slightly off-centre position in the cross-section makes it difficult to clearly visualise the rising bedrock in the Fig. 11. Conversely, borehole FLP-1, despite located in the deeper segment of the aquifer, does not clearly convey that it is located in the concave down region or before the deepening of the bedrock in the cross section. It is important to emphasise that the cross-section was constructed along a specific direction and is based on the interpolated bedrock layer. Therefore, it is plausible that the deepening of the bedrock may manifest itself in a different local direction that is not captured by the current representation of the geological profile.

Indications of potentially stronger inflows are in general more numerous in sediment layers where higher permeability is expected, such as gravel and sandy layers (Fig. 10). However, such inflows also occur in contact with silty and clayey layers, as well as conglomerate layers that can act either as a local barrier to the inflows or as a clear pathway through larger caverns (Fig. 10). The number of potentially stronger inflows in these layers could be lower simply because the proportion of these layers is smaller compared to gravel and sand layers. As the flow logging with the impeller flowmeter was not carried out under pumping conditions, it was not possible to identify the most productive zones and horizontal inflows.

5. Discussion

Of the 13 successfully completed borehole measurements, significant vertical intraborehole flows were observed in 9 of the 12 boreholes tested under ambient conditions. The results indicate that the observed vertical flows in the study area are primarily due to pressure-driven convection. This conclusion is supported by the measurable differences in hydraulic head observed in the monitoring well cluster – BRP-1A, BRP-1B and BRP-1C – and by the camera recordings at PC0–2, which indicate intense recharge from the Sava River.

The three monitoring wells TŠ-1, TŠ-2 and LP-VOD, where no significant vertical intraborehole flow was observed, have a common feature: they are shallower and do not reach the base of the aquifer. This indicates that the vertical flow is more pronounced in deeper monitoring wells that extend to the base of the aquifer or intersect hydrogeologically distinct layers.

All the boreholes analysed in this study are characterised by long screen sections, with most having multiple screen sections separated by shorter non-perforated intermediate casing sections. Only two boreholes, PLIT-1 and BRP-1A, have screen intervals of 6 m or less, with the length of the intermediate cased sections limited to 1–3 m. The remaining boreholes have screen lengths of more than 10 m, with the average between 16 and 24 m and can reach up to 35 m. Of particular note is PC0–2, which is fully equipped with a 60 m long screen section. This borehole had the highest net impeller velocity response among all the boreholes analysed in the study. This observation is consistent with the conclusions of (McMillan et al., 2014), who showed that longer screens increase the magnitude of vertical flows as the head difference between opposite ends of the screen is greater. Nevertheless, it is important to point out that the length of the screen intervals alone is not the primary determinant of higher flow velocities in our study, as can be concluded from the comparison of the length of the screen intervals with the measured impeller velocities. The non-perforated intermediate sections do not separate different layers of the aquifer, as this is a relatively uniform porous medium without significant aquitard layers. In contrast, the short intermediate casing sections connect different screen sections, which in turn act as a single long screen interval.

Based on the geological interpretation, it was found that the direction of intraborehole vertical flows is primarily related to the shape of the base of the aquifer. The downward water flows are significantly related to the local deepening of the bedrock, while the upward flows are related to the local rise of the bedrock. A strong correlation was found between the mean net impeller velocity (rpm) and the calculated vertical water velocity (m/min) for the corresponding segments, which suggests that the velocities were obtained in the correct order of magnitude. However, it is worth noting that of the 12 boreholes in which the logging with the impeller flowmeter was successfully performed and analysed, 8 boreholes have the same casing diameter. We assume that the deviations could be larger if the borehole casing diameters were different. Considering the location and trace of the inferred faults within the study area, they do not appear to play a decisive role in the interpretation of intraborehole flows.

The geological interpretation and measurable differences in hydraulic head observed in monitoring well cluster BRP-1A, BRP-1B, and BRP-1C indicate that the directions and relative velocities of intraborehole flows are closely related to the general vertical groundwater flow in the aquifer. While several studies have modelled and simulated intraborehole flows, particularly in the context of contaminant transport modelling (Elçi et al., 2003; Ma et al., 2011; McMillan et al., 2014; Poulsen et al., 2019a), none have explicitly defined the relationships between vertical water flow velocities within boreholes and those in the surrounding aquifer. It is noteworthy that flow velocities within boreholes can be significantly higher than those in the aquifer (Elçi et al., 2003). Therefore, a modelling approach is required in future studies to assess possible correlations.

The boreholes investigated in this study are not located in the immediate vicinity of the well fields, so it is unlikely that the vertical hydraulic gradients or hydraulic head differences are caused by regional drawdown produced by pumping. Due to the high

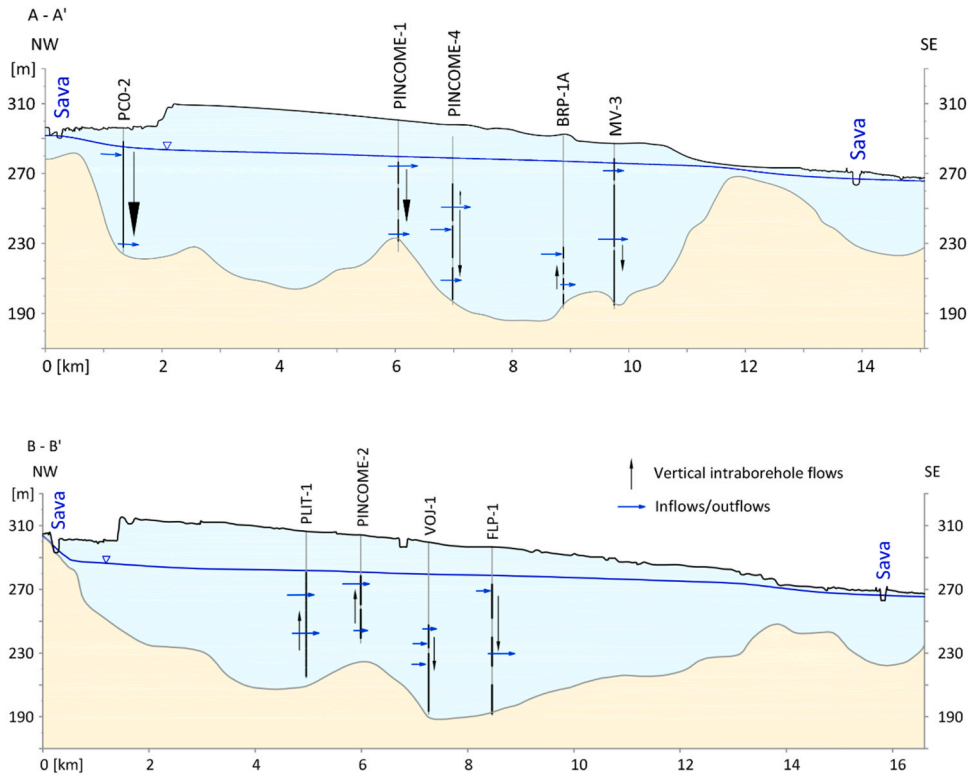

Fig. 11. Two aquifer cross-sections along the main groundwater flowlines: A-A′ and B-B′. The y-axis is vertically exaggerated by a factor of 30 relative to x-axis.

permeability of the aquifer, the same is most likely true for localised increases in recharge due to water infiltration and potential losses from linear infrastructure (e.g. pipelines, waste water pipes) and stormwater catchment areas. However, in order to analyse this aspect, the observations should be seasonal and take into account key factors such as the water level of the Sava River, the recharge regime from the Sava River and precipitation, as well as the succession of dry and rainy periods.

Within the scope of our study, the logging measurements were only repeated in PLIT-1 under different hydrogeological conditions. The groundwater level was 1.48 m higher before the measurements in 2023 than in 2022, which is a relatively significant difference for the given aquifer, considering that the groundwater level fluctuates on average by 2–3 m under different hydrogeological conditions (Janža et al., 2020, 2011). Despite these differences, we consistently observed an upward water flow in both years, especially within the 49–62 m depth segment. However, in 2023, when the groundwater level was higher, the apparent velocity of vertical water flow was also about 1.8 m/min higher. The variability of vertical water gradients within the borehole under different hydrological conditions requires further testing to prove and refine possible correlations and conclusions.

Groundwater samples at the local level are often collected using a 2-inch submersible pump with typical pumping rates reaching up to 0.2 l/s. This flow rate is significantly lower than most of the absolute maximum intraborehole flows (Q_w) measured in this study (Table 2). McMillan et al. have shown through numerical modelling that the ambient intraborehole flows can have a decisive influence on the origin of the samples (McMillan et al., 2014). According to their results, it is possible to overcome the ambient vertical gradients if the maximum ambient flow in the borehole is < 5 % of the pumping rate. However, the sample becomes increasingly biassed towards the zone of highest head intersecting the screen as the ambient flow in the borehole increases towards 50 % of the pumping rate (McMillan et al., 2014). If the ambient flow is much greater than the pumping rate, the sample will be entirely biassed towards the zone with the highest head (McMillan et al., 2014). According to (Poulsen et al., 2019a), the pumping rate must be at least one order of magnitude higher than the intraborehole flow rate to minimise the sample bias. Therefore, the reliability of groundwater samples from boreholes with significant intraborehole flows is questionable if conventional methods (no depth-discrete sampling) were used for sampling.

The main inflows to the boreholes were identified through a comprehensive analysis integrating flowmeter and hydrochemical logs. The analysis suggests that the inflows are more numerous in geological layers where higher permeability is expected, such as gravel and sandy gravel layers, but they also occur in contact with silty, clayey and conglomeratic layers. While the analysis of the geological profiles has proven to be highly valuable for delineating the base of the aquifer, the intermediate inventories remain questionable due to inconsistencies resulting from the different classification methods, leading to superficialities and errors influenced by subjective factors. This emphasises the importance of adhering to appropriate soil classification standards when drilling boreholes. In order to verify and quantitatively assess horizontal inflows under ambient conditions, additional investigations using other methods

such as the point dilution test or similar would be required.

The groundwater temperature in boreholes does not increase with depth, but remains relatively constant and even decreases to a certain extent in most boreholes. This phenomenon is consistent with the results of research on shallow geothermal energy in the City of Ljubljana (Janža et al., 2017) and has also been reported in other regions (Dong et al., 2018; Taniguchi et al., 1999; Ziagos and Blackwell, 1986). Negative temperature gradients may indicate recharge areas, as reported by (Dong et al., 2018; Taniguchi et al., 1999), while (Ziagos and Blackwell, 1986) attributed such temperature inversions to fluid flow in highly conductive fractures and aquifers. The elevated or disturbed temperatures in the upper part of the aquifer can also be influenced by local groundwater inflows and anthropogenic heat sources in the urban area (Janža et al., 2017), which include open-loop geothermal systems (Koren and Janža, 2019), potential losses from linear infrastructure such as pipelines, waste water conduits (Janža et al., 2020) and rainwater infiltration systems.

Previous multi-level groundwater temperature measurements conducted in the City of Ljubljana (Janža et al., 2017) revealed that only one of the nine analysed boreholes exhibited a clear positive temperature gradient. Precisely this borehole is located outside our study area in an aquifer with lower-permeability (Ljubljansko barje), where the groundwater velocity is lower. All other boreholes showed either no significant vertical temperature gradient or a negative gradient. The absence of a positive temperature gradient with depth can likely be attributed to the pressure-driven intraborehole flow or strong advective transport within the highly productive aquifer, which effectively disperses the heat-flow density. This effect is assumed to be more pronounced in highly productive aquifers and boreholes with longer screens, where intraborehole flow velocities are higher.

There are many different methods for estimating vertical groundwater flow within an aquifer, and many of them are based on measurements of temperature or environmental tracer data collected in boreholes (Irvine et al., 2017; Lin et al., 2022; Rusli et al., 2023). Special consideration is required when interpreting temperature or concentration-depth profiles in settings where significant intraborehole flows may occur, as these can distort the representation of actual conditions in the aquifer.

6. Conclusions

The study focused on analysing the characteristics and variability of intraborehole water flows under ambient conditions in a single alluvial aquifer. The aim was to improve our understanding of the intraborehole flow patterns in relation to the technical features of the boreholes and the geological composition of the aquifer. The impeller flowmeter proved to be a reliable tool for assessing the direction and velocity of intraborehole flows in highly productive aquifers, while hydrochemical logs provided a valuable complementary method for identifying zones of potentially stronger inflows. The intraborehole flows in the study area were found to be primarily related to the pressure-driven convection, i.e. differences in hydraulic head between the upper and lower parts of the aquifer. These flows are most pronounced in deeper boreholes and are influenced by the length of the screen sections. Intraborehole flows were observed in geological layers of varying permeability, although they were found to be primarily related to the shape of the base of the aquifer. The downward vertical water flows are associated with a local deepening of the bedrock, while minor upward flows are associated with a local rise of the bedrock. The strongest vertical downward flow was observed in the primary groundwater recharge zone from the Sava River, which coincides with the deepening of the bedrock. On the other hand, stronger vertical upward flows expected in the discharge zones could not be confirmed as there were no tested boreholes close to the groundwater draining into the river. It is assumed that the intraborehole flows have a significant influence on the origin of the groundwater samples, which emphasises the importance of depth-discrete sampling in similar aquifer systems.

CRediT authorship contribution statement

Mihael Brenčič: Writing – review & editing, Supervision, Methodology. **Simon Mozetič:** Writing – review & editing, Data curation. **Joerg Prestor:** Writing – review & editing, Methodology, Funding acquisition, Formal analysis, Conceptualization. **Janja Svetina:** Writing – review & editing, Writing – original draft, Visualization, Methodology, Formal analysis, Conceptualization.

Declaration of Competing Interest

The authors declare that they have no known competing financial interests or personal relationships that could have appeared to influence the work reported in this paper.

Acknowledgments

The research was funded by the Slovenian Research and Innovation Agency (ARIS) through research program P1–0020 Groundwater and Geochemistry in the frame of the Young Researchers programme and by the Interreg Central Europe project MAURICE.

Data availability

Data will be made available on request.

References

ARSO, 2024. Lidar GIS viewer [WWW Document]. URL https://gis.arso.gov.si/evode/profile.aspx?id=atlas_voda_Lidar@Arso&culture=en-US&AspxAutoDetectCookieSupport= 1 (accessed 10.2.24).

Atanackov, J., Jamšek Rupnik, P., Jež, J., Celarc, B., Novak, M., Milanič, B., Markelj, A., Bavec, M., Kastelic, V., 2021. Database of Active Faults in Slovenia: Compiling a New Active Fault Database at the Junction Between the Alps, the Dinarides and the Pannonian Basin Tectonic Domains. Frontiers in Earth Science 9. https://doi.org/10.3389/feart.2021.604388.

Barahona-Palomo, M., Riva, M., Sanchez-Vila, X., Vazquez-Sune, E., Guadagnini, A., 2011. Quantitative comparison of impeller-flowmeter and particle-size-distribution techniques for the characterization of hydraulic conductivity variability. Hydrogeol. J. 19, 603–612. https://doi.org/10.1007/s10040-011-0706-5.

Berthold, S., 2010. Synthetic Convection Log — characterization of vertical transport processes in fluid-filled boreholes. J. Appl. Geophys. 72, 20–27. https://doi.org/10.1016/j.jappgeo.2010.06.007.

Berthold, S., Börner, F., 2008. Detection of free vertical convection and double-diffusion in groundwater monitoring wells with geophysical borehole measurements. Environ. Geol. 54, 1547–1566. https://doi.org/10.1007/s00254-007-0936-y.

Börner, F., Berthold, S., 2009. Vertical flows in groundwater monitoring wells. In: Kirsch, R. (Ed.), Groundwater Geophysics. Springer Berlin Heidelberg, Berlin, Heidelberg, pp. 367–389. https://doi.org/10.1007/978-3-540-88405-7_13.

Cermak, V., Safanda, J., Bodri, L., 2008. Precise temperature monitoring in boreholes: evidence for oscillatory convection? Part 1: experiments and field data. Int. J. Earth Sci. 97, 365–373. https://doi.org/10.1007/s00531-007-0237-4.

Datel, J.V., Kobr, M., Prochazka, M., 2009. Well logging methods in groundwater surveys of complicated aquifer systems: bohemian Cretaceous Basin. Environ. Geol. 57, 1021–1034. https://doi.org/10.1007/s00254-008-1388-8.

Demezhko, D.Yu, Mindubaev, M.G., Khatskevich, B.D., 2017. Thermal effects of natural convection in boreholes. Russ. Geol. Geophys. 58, 1270–1276. https://doi.org/10.1016/j.rgg.2016.10.016.

Domenico, P.A., Schwartz, F.W., 1998. Physical and chemical hydrogeology, 2nd ed. Wiley, New York.

Dong, L., Fu, C., Liu, J., Wang, Y., 2018. Disturbances of temperature-depth profiles by surface warming and groundwater flow convection in Kumamoto Plain, Japan. Geofluids 2018, 1–14. https://doi.org/10.1155/2018/8451276.

Elçi, A., Molz, F.J., Waldrop, W.R., 2001. Implications of Observed and Simulated Ambient Flow in Monitoring Wells. Groundwater 39, 853–862. https://doi.org/10.1111/j.1745-6584.2001.tb02473.x.

Elçi, A., Flach, G.P., Molz, F.J., 2003. Detrimental effects of natural vertical head gradients on chemical and water level measurements in observation wells: identification and control. J. Hydrol. 281, 70–81. https://doi.org/10.1016/S0022-1694(03)00201-4.

Eppelbaum, L.V., Kutasov, I.M., 2011. Estimation of the effect of thermal convection and casing on the temperature regime of boreholes: a review. J. Geophys. Eng. 8, R1–R10. https://doi.org/10.1088/1742-2132/8/1/R01.

Fricke, S., Schön, J., 1999. Praktische Bohrlochgeophysik. Enke im Georg Thieme Verlag, Stuttgart.

Grad, K., & Ferjančič, L., 1968. Basic geological map of Yugoslavia 1:100000 - sheet Kranj. In *https://egeologija.si/*. Geološki zavod Ljubljana. https://egeologija.si/geonetwork/srv/eng/catalog.search#/metadata/9240b8ee-8d69-4cd0-a696-a53b39cfd886.

Hearst, J.R., Nelson, P.H., Paillet, F.L., 2000. Well logging for physical properties: a handbook for geophysicists, geologists, and engineers, 2nd ed. Wiley, Chichester, New York.

Hess, A.E., 1986. Identifying hydraulically conductive fractures with a slow-velocity borehole flowmeter. Can. Geotech. J. 23, 69–78. https://doi.org/10.1139/t86-008.

Irvine, D.J., Kurylyk, B.L., Cartwright, I., Bonham, M., Post, V.E.A., Banks, E.W., Simmons, C.T., 2017. Groundwater flow estimation using temperature-depth profiles in a complex environment and a changing climate. Sci. Total Environ. 574, 272–281. https://doi.org/10.1016/j.scitotenv.2016.08.212.

Jamnik, B., Žitnik, M., 2021. Annual report on the compliance of drinking water in the supply areas managed by the public company Vodovod Kanalizacija Snaga d.o.o. in 2020 (in Slovene).

Jamnik, B., Žitnik, M., 2022. Annual report on the compliance of drinking water in the supply areas managed by the public company Vodovod Kanalizacija Snaga d.o.o. in 2021 (in Slovene).

Jamnik, B., Janža, M., Smrekar, A., Breg Valjavec, M., Cerar, S., Cosma, C., Hribernik, K., Krivic, M., Meglič, P., Pestotnik, S., Piepenbrink, M., Podboj, M., Polajnar Horvat, K., Prestor, J., Schüth, C., Šinigoj, J., Šram, D., Urbanc, J., Žibret, G., 2014. Skrb za pitno vodo, Geografija Slovenije. ZRC SAZU, Založba ZRC. https://doi.org/10.3986/9789610503637.

Janža, M., 2015. A decision support system for emergency response to groundwater resource pollution in an urban area (Ljubljana, Slovenia). Environ. Earth Sci. 73, 3763–3774. https://doi.org/10.1007/s12665-014-3662-2.

Janža, M., Meglič, P., Šram, D., 2011. Numerical hydrological modeling (project INCOME action report).

Janža, M., Lapanje, A., Šram, D., Rajver, D., Novak, M., 2017. Research of the geological and geothermal conditions for the assessment of the shallow geothermal potential in the area of Ljubljana, Slovenia. Geologija 60, 309–327. https://doi.org/10.5474/geologija.2017.022.

Janža, M., Prestor, J., Pestotnik, S., Jamnik, B., 2020. Nitrogen mass balance and pressure impact model applied to an urban aquifer. Water 12, 1171. https://doi.org/10.3390/w12041171.

Kelly, W.E., Mareš, S., Karous, M., 1993. Applied geophysics in hydrogeological and engineering practice. Developments in water science. Elsevier, Amsterdam New York.

Keys, W.S., 1990. Borehole Geophysics Applied to Ground-Water Investigations, Techniques of Water-Resources Investigations. United States Government Printing Office; For sale by the Books and Open-File Reports Section. U.S. Geological Survey.

Keys, W.S., 1997. A practical guide to borehole geophysics in environmental investigations. CRC Press, Boca Raton.

Kolar-Jurkovšek, T., 2007. Late Carboniferous flora of Castle Hill in Ljubljana (Slovenia). Geologija 50, 9–18. https://doi.org/10.5474/geologija.2007.001.

Koren, K., Janža, M., 2019. Risk assessment for open loop geothermal systems, in relation to groundwater chemical composition (Ljubljana pilot area, Slovenia). Geologija 62, 237–249. https://doi.org/10.5474/geologija.2019.011.

Lin, Y.-F., Chang, C.-H., Tsai, J.-P., 2022. Analytical solution for estimating transient vertical groundwater flux from temperature-depth profiles. J. Hydrol. 610, 127920. https://doi.org/10.1016/j.jhydrol.2022.127920.

Ma, R., Zheng, C., Tonkin, M., Zachara, J.M., 2011. Importance of considering intraborehole flow in solute transport modeling under highly dynamic flow conditions. J. Contam. Hydrol. 123, 11–19. https://doi.org/10.1016/j.jconhyd.2010.12.001.

Mayo, A.L., 2010. Ambient well-bore mixing, aquifer cross-contamination, pumping stress, and water quality from long-screened wells: What is sampled and what is not? Hydrogeol. J. 18, 823–837. https://doi.org/10.1007/s10040-009-0568-2.

McMillan, L.A., Rivett, M.O., Tellam, J.H., Dumble, P., Sharp, H., 2014. Influence of vertical flows in wells on groundwater sampling. J. Contam. Hydrol. 169, 50–61. https://doi.org/10.1016/j.jconhyd.2014.05.005.

Medici, G., Munn, J.D., Parker, B.L., 2024. Delineating aquitard characteristics within a Silurian dolostone aquifer using high-density hydraulic head and fracture datasets. Hydrogeol. J. 32, 1663–1691. https://doi.org/10.1007/s10040-024-02824-9.

Molz, F.J., Morin, R.H., Hess, A.E., Melville, J.G., Güven, O., 1989. The Impeller Meter for measuring aquifer permeability variations: evaluation and comparison with other tests. Water Resour. Res. 25, 1677–1683. https://doi.org/10.1029/WR025i007p01677.

Molz, F.J., Boman, G.K., Young, S.C., Waldrop, W.R., 1994. Borehole flowmeters: field application and data analysis. J. Hydrol. 163, 347–371. https://doi.org/10.1016/0022-1694(94)90148-1.

Molz, F.L., Young, S.C., 1993. Development and application of borehole flowmeters for environmental assessment. Log. Anal. 34.

Munn, J.D., Maldaner, C.H., Coleman, T.I., Parker, B.L., 2020. Measuring fracture flow changes in a bedrock aquifer due to open hole and pumped conditions using active distributed temperature sensing. e2020WR027229 Water Resour. Res. 56. https://doi.org/10.1029/2020WR027229.

Newhouse, M.W., Izbicki, J.A., Smith, G.A., 2005. Comparison of velocity-log data collected using impeller and electromagnetic flowmeters. Groundwater 43, 434–438. https://doi.org/10.1111/j.1745-6584.2005.0030.x.
Oberlander, P.L., Russell, C.E., 2006. Process considerations for trolling borehole flow logs. Groundw. Monit. Remediat. 26, 60–67. https://doi.org/10.1111/j.1745-6592.2006.00084.x.
Paillet, F., Crowder, R., Hess, A., 1996. High-resolution flowmeter logging applications with the heat-pulse flowmeter. J. Environ. Eng. Geophys. 1, 1–11. https://doi.org/10.4133/JEEG1.1.1.
Paillet, F.L., Senay, Y., Mukhopadhyay, A., Szekely, F., 2000. Flowmetering of drainage wells in Kuwait City, Kuwait. J. Hydrol. 234, 208–227. https://doi.org/10.1016/S0022-1694(00)00261-4.
Pauwels, H., Négrel, P., Dewandel, B., Perrin, J., Mascré, C., Roy, S., Ahmed, S., 2015. Hydrochemical borehole logs characterizing fluoride contamination in a crystalline aquifer (Maheshwaram, India). J. Hydrol. 525, 302–312. https://doi.org/10.1016/j.jhydrol.2015.03.017.
Poulsen, D.L., Cook, P.G., Simmons, C.T., Solomon, D.K., Dogramaci, S., 2019b. Depth-resolved groundwater chemistry by longitudinal sampling of ambient and pumped flows within long-screened and open borehole wells. Water Resour. Res. 55, 9417–9435. https://doi.org/10.1029/2019WR025713.
Premru, U., 1980. Basic geological map of Yugoslavia 1:100000 - sheet Ljubljana. In https://egeologija.si/. Geološki zavod Ljubljana. https://egeologija.si/geonetwork/srv/eng/catalog.search#/metadata/c5d86800-e3e3-48d3-ad87-46bfb32620b7.
Poulsen, D.L., Cook, P.G., Simmons, C.T., McCallum, J.L., Dogramaci, S., 2019a. Effects of intraborehole flow on purging and sampling long-screened or open wells. Groundwater 57, 269–278. https://doi.org/10.1111/gwat.12797.
Premru, U., 1983. Basic geological map of SFRY. Interpreter for list Ljubljana: L 33-66 (in Slovene).
Premru, U., Pirc, S., 2005. Tektonika in tektogeneza slovenije: geoloska zgradba in geoloski razvoj slovenije = tectonics and tectogenesis of slovenia. Geoloski zavod Slovenije, Ljubljana.
Robertson Geologging Ltd, 2024. Specification Sheets & User Manuals [WWW Document]. Robertson Geo. URL ⟨https://www.robertson-geo.com/⟩ (accessed 10.2.24).
Rusli, S.R., Weerts, A.H., Mustafa, S.M.T., Irawan, D.E., Taufiq, A., Bense, V.F., 2023. Quantifying aquifer interaction using numerical groundwater flow model evaluated by environmental water tracer data: application to the data-scarce area of the Bandung groundwater basin, West Java, Indonesia. J. Hydrol. Reg. Stud. 50, 101585. https://doi.org/10.1016/j.ejrh.2023.101585.
Schürch, M., Buckley, D., 2002. Integrating geophysical and hydrochemical borehole-log measurements to characterize the Chalk aquifer, Berkshire, United Kingdom. Hydrogeol. J. 10, 610–627. https://doi.org/10.1007/s10040-002-0220-x.
Sellwood, S.M., Hart, D.J., Bahr, J.M., 2015. Evaluating the Use of In-Well Heat Tracer Tests to Measure Borehole Flow Rates. Groundw. Monit. Remediat. 35, 85–94. https://doi.org/10.1111/gwmr.12134.
SIST EN ISO 14688-2:2004, 2004. Geotechnical investigation and testing - Identification and classification of soil - Part 2: Principles for a classification.
Sondex, 2007. Spinner Selection Guide.
Šram, D., Brenčič, M., Lapanje, A., Janža, M., 2012. Perched aquifers spatial model: a case study for Ljubljansko polje (central Slovenia). Geologija 55, 107–116. https://doi.org/10.5474/geologija.2012.008.
Svetina, J., Prestor, J., Jamnik, B., Auersperger, P., Brenčič, M., 2024. Contaminant trends in urban groundwater: case study from Ljubljana (Central Slovenia). Water 16, 890. https://doi.org/10.3390/w16060890.
Taniguchi, M., Shimada, J., Tanaka, T., Kayane, I., Sakura, Y., Shimano, Y., Dapaah-Siakwan, S., Kawashima, S., 1999. Disturbances of temperature-depth profiles due to surface climate change and subsurface water flow: 1. An effect of linear increase in surface temperature caused by global warming and urbanization in the Tokyo Metropolitan Area, Japan. Water Resour. Res. 35, 1507–1517. https://doi.org/10.1029/1999WR900009.
Van Meir, N., Jaeggi, D., Herfort, M., Loew, S., Pezard, P.A., Lods, G., 2007. Characterizing flow zones in a fractured and karstified limestone aquifer through integrated interpretation of geophysical and hydraulic data. Hydrogeol. J. 15, 225–240. https://doi.org/10.1007/s10040-006-0086-4.
Vizintin, G., Souvent, P., Veselič, M., Cencur Curk, B., 2009. Determination of urban groundwater pollution in alluvial aquifer using linked process models considering urban water cycle. J. Hydrol. 377, 261–273. https://doi.org/10.1016/j.jhydrol.2009.08.025.
Ziagos, J.P., Blackwell, D.D., 1986. A model for the transient temperature effects of horizontal fluid flow in geothermal systems. J. Volcanol. Geotherm. Res. 27, 371–397. https://doi.org/10.1016/0377-0273(86)90021-1.
Žlebnik, L., 1971. Pleistocene deposits of the Kranj, Sora and Ljubljana fields. Geologija 14, 5–51.